Ab initio impact ionization rate in GaAs, GaN, and ZnS

Angelika Kuligk, Niels Fitzer, and Ronald Redmer
Universität Rostock, Institut für Physik, D-18051 Rostock, Germany
(Received 25 October 2004; published 4 February 2005)

We have performed extensive *ab initio* band structure calculations within density functional theory using an exact exchange formalism with a local density approximation for correlations. The wave-vector-dependent impact ionization rate is determined for GaAs, GaN, and ZnS. A strong asymmetry of the microscopic scattering rate as well as a pronounced influence of the band structure is found. We present also energy-averaged impact ionization rates which can be used in ensemble Monte Carlo simulations of high-field electron transport in these materials.

DOI: 10.1103/PhysRevB.71.085201 PACS number(s): 71.15.Mb, 72.20.Ht, 71.55.Eq, 71.55.Gs

I. INTRODUCTION

High-field transport in semiconductors has long been a concern in relation to the performance of semiconductor electronic and optoelectronic devices.[1,2] A high-field process of particular interest in semiconductors is the impact ionization rate associated with electron-hole pair excitation due to energetic hot carriers in the conduction or valence bands. Measurements of the ionization coefficient, however, give only information on the field-dependent microscopic scattering rate averaged with the actual nonequilibrium distribution function.[3] Recently, the dynamics of carrier multiplication due to impact ionization has been studied experimentally on ultrashort time scales in $Al_xGa_{1-x}As$ diodes.[4] The microscopic description of this extreme nonequilibrium process remains a demanding task.

The electron initiated impact ionization rate (IIR) was calculated for a variety of semiconductor materials within a full-band approach by using the empirical pseudopotential method (EPM).[5] The influence of quantum and high-field effects on the impact ionization process has been studied as well, in particular the intracollisional field effect[6] and collision broadening.[7,8]

It is found that the band structure has a strong influence on the IIR. Especially, the wave-vector-dependent IIR is sensitive with respect to the details of the band structure in the Brillouin zone, including the location and shape of higher bands. Therefore, instead of using approximate band structures, *ab initio* electronic structure calculations are needed to get reliable results for the IIR. The first calculations in this sense were performed for GaAs and InGaAs within a screened-exchange local density approximation (sX-LDA) of density functional theory (DFT).[9,10]

Here we present results of *ab initio* calculations for the IIR in GaAs, GaN, and ZnS within DFT by using an exact exchange formalism with a local density approximation for correlations (EXX-LDA).[11] The exact treatment of the exchange interaction yields accurate band gap energies, in contrast to the standard LDA which is plagued by the well-known band gap problem.[12] These improved *ab initio* band structures were applied recently for the calculation of the high-field electron transport in GaAs and ZnS using full-band ensemble Monte Carlo simulations; good agreement with experimental data was achieved.[13]

II. BAND STRUCTURE

The electron structure calculations using DFT within the EXX-LDA were performed as outlined in Refs. 11 and 12. The local Kohn-Sham exchange potential V_x is treated exactly, while the correlation contributions are considered within the LDA Perdew-Zunger parametrization.[14] All calculations use consistent norm-conserving Troullier-Martins-type EXX-LDA pseudopotentials[15] in the Kleinman-Bylander form[16] and were carried out at the experimental lattice constants. The energy cutoffs are 23 Ry for GaAs, 40 Ry for GaN, and 60 Ry for ZnS. The band structure is calculated at 916 points in the irreducible wedge of the Brillouin zone. In addition, for the density of states we use 2573 points. The $3d$ electrons were always treated as part of the frozen core.

The resulting band structures and densities of states (DOS) are shown in Figs. 1–3 in comparison with EPM calculations. The sets of EPM parameters used here for GaAs are given in Ref. 17 and for GaN and ZnS in Ref. 18, respectively. Previous EPM calculations for GaAs (Refs. 19 and 20) are in very good overall agreement with the EXX-LDA results shown in Fig. 1 so that the use of empirical pseudopotentials is well founded for this material. This is not the case for GaN and ZnS where significant deviations between the EPM and EXX-LDA band structures occur, even for the lowest conduction band and the highest valence band. Furthermore, the DOS extracted from these band structures is considerably different, especially the location and height of the maxima.

III. IMPACT IONIZATION RATE

A. Computational scheme

In the process of impact ionization, an energetic conduction band electron impact ionizes a valence band electron, i.e., $1+2\rightarrow 3+4$, see Fig. 4. The states i represent the band index n_i and the energy $\varepsilon_{n_i}(\mathbf{k}_i)$. The band indices and energies $n_1,\varepsilon_{n_1}(\mathbf{k}_1),n_3,\varepsilon_{n_3}(\mathbf{k}_3),n_4,\varepsilon_{n_4}(\mathbf{k}_4)$ run over the conduction bands, while $n_2,\varepsilon_{n_2}(\mathbf{k}_2)$ belong to the valence bands. We apply Fermi's golden rule to evaluate the IIR,[21]

 ©2005 The American Physical Society

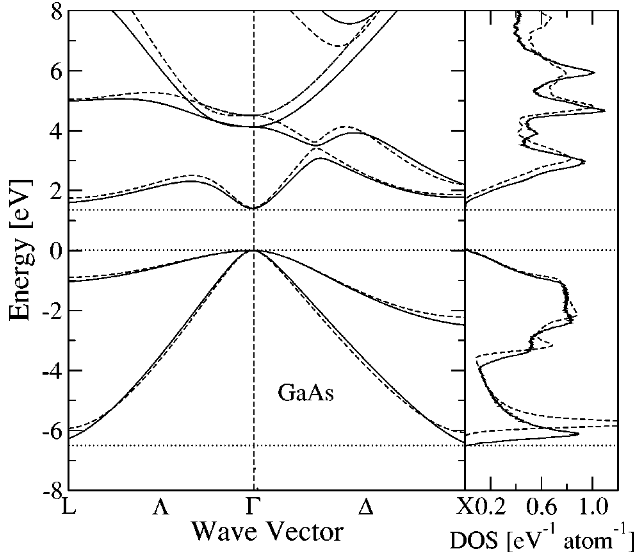

FIG. 1. Band structure and density of states for GaAs using DFT in EXX-LDA (solid lines) and the EPM (broken lines).

$$r_{ii}(1) = -\frac{4}{\hbar^2}\sum_{2,3,4} |M_{\mathrm{tot}}(1,2;3,4)|^2 \times \delta(\varepsilon(3)+\varepsilon(4)-\varepsilon(1)-\varepsilon(2)), \qquad (1)$$

where the total matrix element contains direct, exchange, and umklapp processes via

$$|M_{\mathrm{tot}}|^2 = 2|M_d|^2 + 2|M_e|^2 - (M_d^* M_e + M_d M_e^*). \qquad (2)$$

The matrix elements with $M_e(1,2;3,4)=M_d(1,2;4,3)$ are given by

$$M_d(1,2;3,4) = \int d^3r \int d^3r' \Psi^*_{n_4}(\mathbf{k}_4,\mathbf{r}')\Psi^*_{n_3}(\mathbf{k}_3,\mathbf{r}) \times v(\mathbf{r}-\mathbf{r}',\omega)\Psi_{n_1}(\mathbf{k}_1,\mathbf{r})\Psi_{n_2}(\mathbf{k}_2,\mathbf{r}'). \qquad (3)$$

The Bloch wave functions for the electrons are $\Psi_n(\mathbf{k},\mathbf{r})$

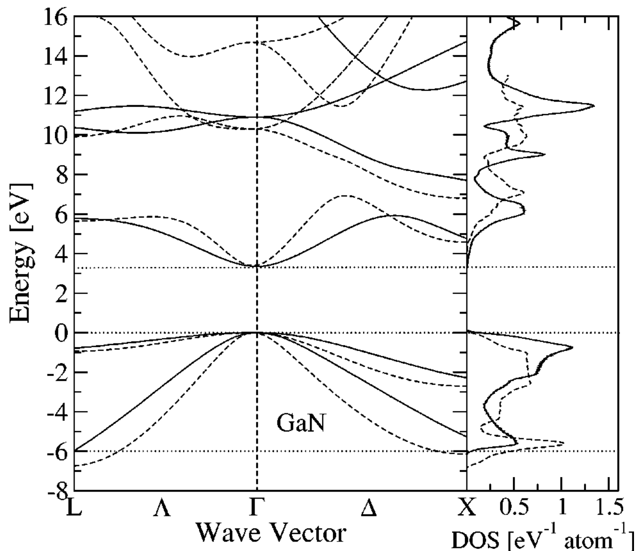

FIG. 2. Same as in Fig. 1 but for GaN.

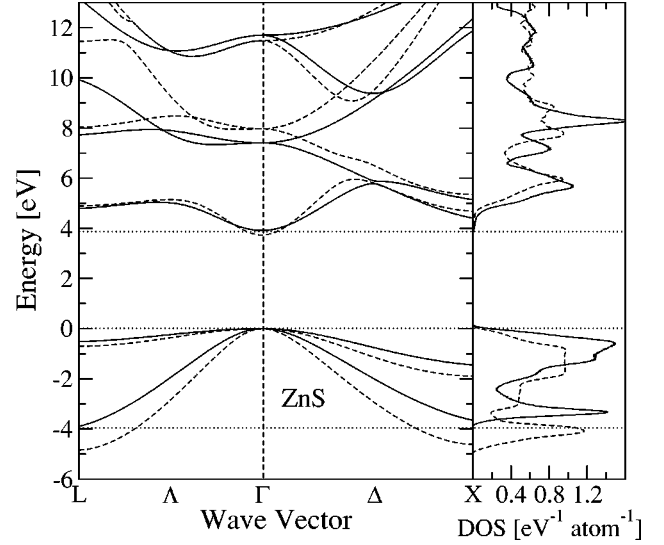

FIG. 3. Same as in Fig. 1 but for ZnS.

$=(1/\sqrt{\Omega})\exp(i\mathbf{k}\cdot\mathbf{r})u_n(\mathbf{k},\mathbf{r})$; Ω is the crystal volume. The Coulomb interaction

$$v(\mathbf{r}-\mathbf{r}',\omega) = \int \frac{d^3q}{(2\pi)^3} v(\mathbf{q},\omega)\exp[i\mathbf{q}\cdot(\mathbf{r}-\mathbf{r}')] \qquad (4)$$

is screened via the dielectric function $\epsilon(\mathbf{q},\omega)$,

$$v(\mathbf{q},\omega) = \frac{e^2}{\epsilon_0 \epsilon(\mathbf{q},\omega)\mathbf{q}^2}, \qquad (5)$$

where ϵ_0 is the static dielectric constant. We have used the model dielectric function of Levine and Louie.[22] For direct processes we have

$$|M_d|^2 = \sum_{\mathbf{G}} \left| \sum_{\mathbf{G}'} \frac{e^2 B^{(\mathbf{G}')}_{n_1 n_3}(\mathbf{k}_1,\mathbf{k}_3) B^{(\mathbf{G}-\mathbf{G}')}_{n_2 n_4}(\mathbf{k}_2,\mathbf{k}_4)}{\epsilon_0 \epsilon(\mathbf{q},\omega)\mathbf{q}^2} \right|^2 \times \delta_{\mathbf{k}_1+\mathbf{k}_2,\mathbf{k}_3+\mathbf{k}_4+\mathbf{G}}. \qquad (6)$$

The Bloch integrals

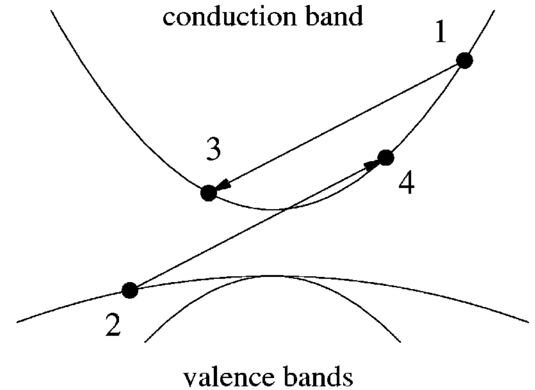

FIG. 4. Schematic impact ionization process for electrons.

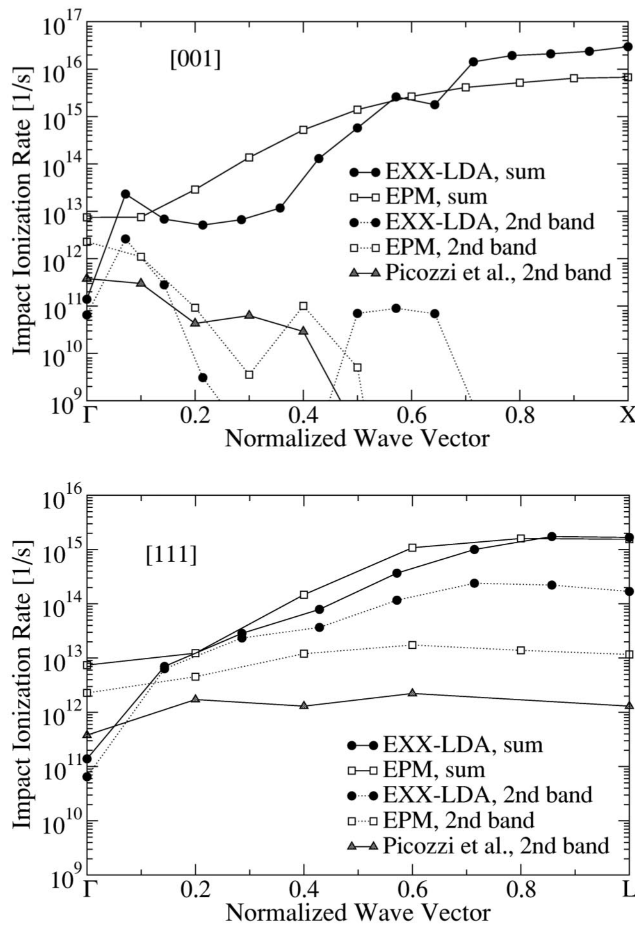

FIG. 5. Wave-vector dependent IIR for GaAs along the $\Gamma-X$ [001] and $\Gamma-L$ [111] direction. We compare the EXX-LDA and EPM contributions of the second conduction band with respective sX-LDA results of Picozzi *et al.* (Ref. 9).

$$B^{(\mathbf{G})}_{n_i n_j}(\mathbf{k}_i,\mathbf{k}_j) = \frac{1}{\Omega}\int d^3r \exp(i\mathbf{G}\cdot\mathbf{r})u^*_{n_j}(\mathbf{k}_j,\mathbf{r})u_{n_i}(\mathbf{k}_i,\mathbf{r}) \quad (7)$$

are defined by the Bloch factors $u_n(\mathbf{k},\mathbf{r})$ which are calculated by an expansion with respect to reciprocal lattice vectors $\mathbf{G}$. We have considered 113 reciprocal lattice vectors with $|\mathbf{G}| \leqslant \sqrt{20}(2\pi/a)$. Higher expansion coefficients were determined within perturbation theory[23] if necessary to reach convergence. Momentum and energy transfer are defined as $\mathbf{q} = \mathbf{k}_1 - \mathbf{k}_3 + \mathbf{G}'$ and $\hbar\omega = \varepsilon_{n_1}(\mathbf{k}_1) - \varepsilon_{n_3}(\mathbf{k}_3)$, respectively. We consider umklapp processes up to the sixth order in $\mathbf{G}'$.

The wave-vector-dependent IIR defined by Eq. (1) can be averaged over the entire Brillouin zone to obtain an energy dependent rate $R(E)$ according to

$$R(E) = \frac{\sum_{n_1,\mathbf{k}_1} r_{ii}(n_1,\mathbf{k}_1)\,\delta[E-\varepsilon_{n_1}(\mathbf{k}_1)]}{\sum_{n_1,\mathbf{k}_1}\delta[E-\varepsilon_{n_1}(\mathbf{k}_1)]}, \quad (8)$$

which is often used in Monte Carlo simulations of high field-electron transport in semiconductors. This scattering rate can be approximated by an interpolation formula

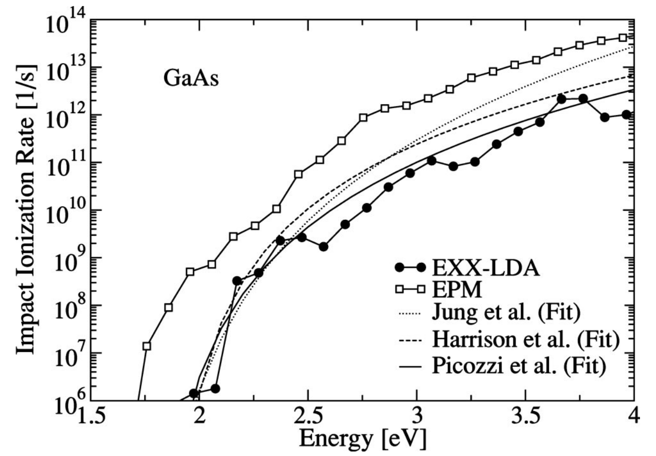

FIG. 6. IIR for GaAs using EXX-LDA (solid circles) and EPM (open boxes) band structures in comparison with other results [Picozzi *et al.* (Ref. 9), Jung *et al.* (Ref. 27), Harrison *et al.* (Ref. 28)] parametrized via Eq. (9).

$$R^{\mathrm{Fit}}(E) = P(E-E_{\mathrm{th}})^a. \quad (9)$$

The prefactor P, the threshold energy E_{th}, and the power a are parameters adjusted to the numerical data. The original Keldysh formula[24] with $a=2$ is derived within the parabolic band approximation using effective masses.

Previous calculations of the IIR have indicated that pronounced contributions arise from higher conduction bands, especially in wide bandgap materials. Furthermore, a marked anisotropy in $\mathbf{k}$ space is obtained which derives from the restrictions imposed by the conservation of energy and momentum. We have taken into account four conduction and four valence bands for the complete numerical evaluation of the IIR given by Eq. (1), processing the EXX-LDA as well as the EPM band structures shown in Figs. 1–3.

The integrals in Eq. (1) extend over the entire Brillouin zone and are evaluated using an efficient numerical procedure developed by Sano and Yoshii.[25] Making extensive use of symmetry relations imposed by the crystal structure, the integrations can be restricted to the irreducible wedge of the Brillouin zone where a large number of points can be taken into account for the numerical evaluation. We have considered here 356 points in the irreducible wedge which correspond to a total of 11 901 points in the Brillouin zone so that a reasonable convergence of the numerical results is warranted.

B. Results for GaAs

First, the wave-vector-dependent IIR is shown for GaAs in Fig. 5. A strong asymmetry along the directions in the Brillouin zone and marked differences between the EXX-LDA and EPM results are clearly to be seen, especially in the Γ valley. For example, the contributions of the second conduction band as given in the sX-LDA calculation[9] are compared. Pronounced differences, especially in the [111] direction, occur which underline the strong influence of the band structure on the IIR. Notice that the total rate is mainly determined by contributions of the third and fourth conduction band.

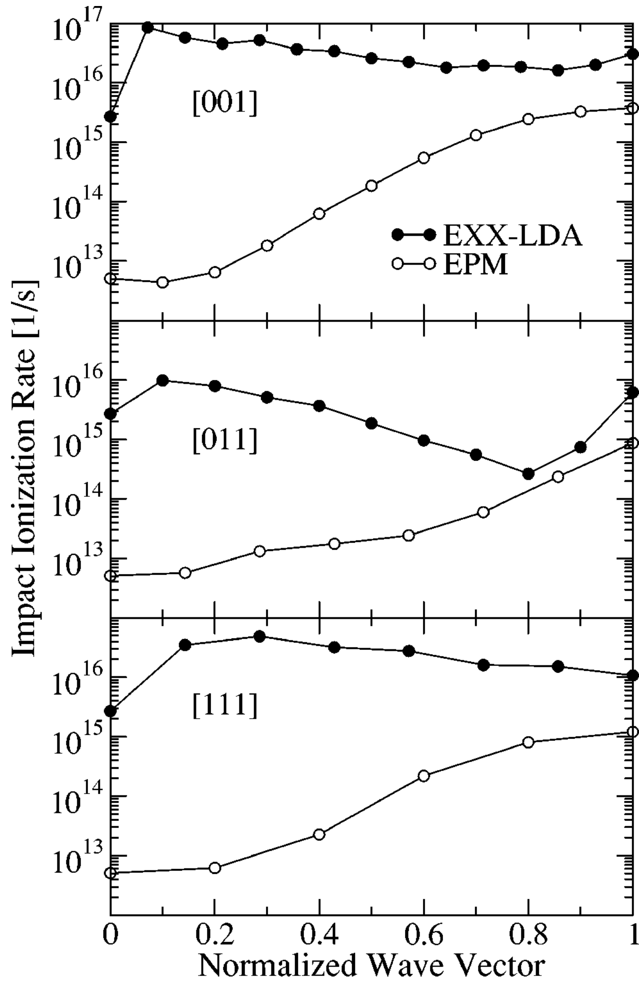

FIG. 7. IIR along the high-symmetric lines in GaN by using the EPM and EXX-LDA band structures.

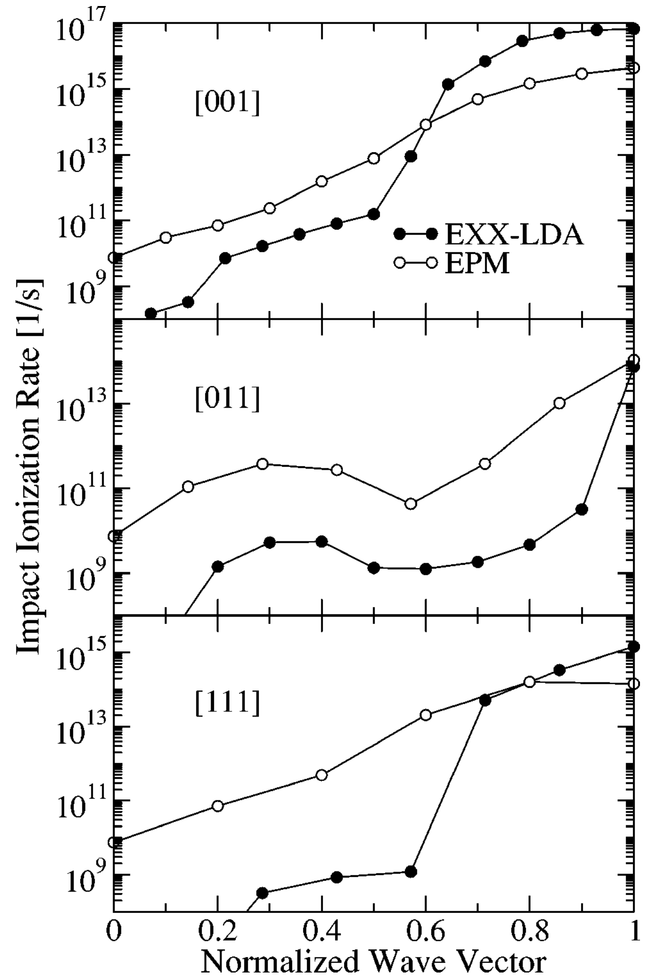

FIG. 8. Same as in Fig. 7 but for ZnS.

The total energy-averaged IIR according to Eq. (8) is shown for GaAs in Fig. 6.[26] The EXX-LDA and EPM results are compared with other EPM-based calculations.[27,28] A good agreement is found with the sX-LDA results[9] although only three conduction bands were included in this evaluation. The IIR derived from the present EPM band structure has a lower threshold and is in general too high by 1–2 orders of magnitude. Notice that an average of the **k**-dependent IIR along the highly symmetric lines as performed earlier[17] yields a higher threshold than the average according to Eq. (8) but almost the same values for higher energies. The other EPM-based calculations for the IIR (Refs. 27 and 28) give the same threshold behavior as the *ab initio* results, but higher rates for higher energies.

C. Results for GaN and ZnS

The wave-vector-dependent IIR for GaN and ZnS is shown along the high-symmetric lines in Figs. 7 and 8, respectively. Strongly different rates are obtained from the EPM and EXX-LDA band structures in all three directions. For GaN, the EXX-LDA results are 3–4 orders of magnitude higher than the EPM rates near the Γ valley, while the differences become smaller at the edge of the Brillouin zone. For ZnS, the EPM rates are generally higher by 1–2 orders of magnitude except at the X valley in [001] direction where by far the highest rates are derived from the EXX-LDA band structure.

Because of the large band gap, impact ionization processes in these materials can only be generated by electrons in the higher bands. Looking at the EXX-LDA band structures in Figs. 2 and 3 in more detail, the main contributions to the IIR in GaN arise from the second to fourth conduction band near the Γ valley in the L and X direction. In ZnS, the third and fourth band give the main contributions in the X direction at the edge of the Brillouin zone; the second band is still too low at the Γ point.

The results for the energy-averaged IIR for GaN and ZnS are shown in Figs. 9 and 10, respectively. The threshold energies amount to 4.0 eV for GaN and 3.7 eV for ZnS, slightly smaller than the EPM values. We find a strong increase of the IIR at about 5.75 eV (GaN) and 4.75 eV (ZnS), much more pronounced than the EPM results in that region. In the following energy domain, the rate based on the EXX-LDA is for both materials considerably higher than the EPM rate. The curve of Kolnik *et al.*[29] for GaN was derived by applying a Monte Carlo method for the evaluation of the integrals in Eq. (1) and an EPM band structure. A relatively soft threshold behavior is obtained from this approach.

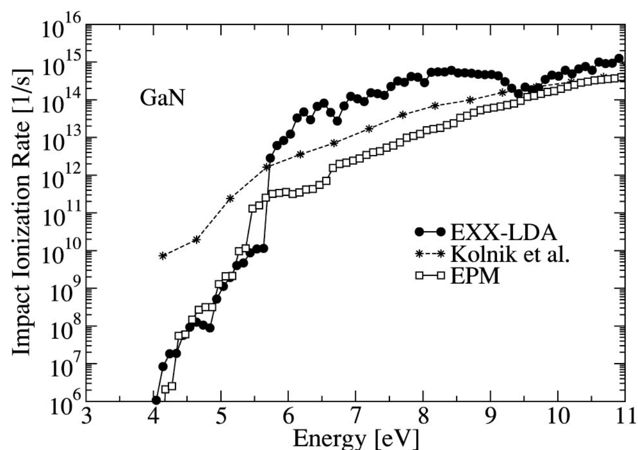

FIG. 9. Same as in Fig. 6 but for GaN. We compare with EPM results of Kolnik *et al.* (Ref. 29).

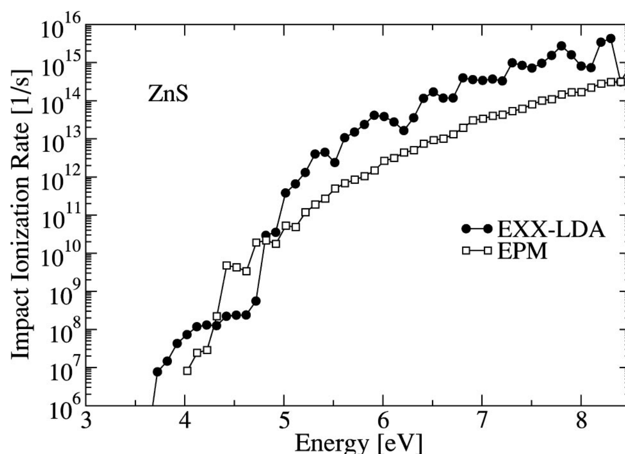

FIG. 10. Same as in Fig. 6 but for ZnS.

It is interesting to correlate the peaks and minima of the DOS with the structures of the IIR for both materials. The first peak of the DOS owing to the first conduction band gives no contributions to the IIR in both cases because it is located below the threshold energy. The position of the second peak of the DOS in GaN just coincides with the sharp increase of the IIR at 5.75 eV. The second peak of the DOS in ZnS, however, is still below the threshold energy for impact ionization and does not contribute. Only the third peak is close to the threshold in this material while the strong increase at 4.75 eV occurs in a region with an almost constant but high DOS of about $0.5(\mathrm{eV\,atom})^{-1}$. The DOS in GaN is generally smaller than in ZnS and has a more pronounced peak structure which is then more apparent in the IIR.

IV. CONCLUSION

In summary, we have performed *ab initio* band structure calculations for GaAs, GaN, and ZnS using DFT within the EXX-LDA in order to compute the microscopic IIR. We have shown that the IIR is strongly sensitive with respect to the band structure and asymmetric in **k**-space. We find a strong increase above the threshold energy at about 5.75 eV (GaN) and 4.75 eV (ZnS). A correlation to the structures of the DOS can be given for GaN while for ZnS a constant but high DOS occurs in that region. These new results for the IIR can be applied in Monte Carlo simulations of the high-field electron transport (see, e.g., Refs. 13, 19, 29, and 30) in order to gain more insight into the process of carrier multiplication in semiconductors.

ACKNOWLEDGMENTS

We thank S. M. Goodnick, E. E. Krasovskii, A. Leitenstorfer, W. Schattke, E. Schöll, M. Städele, and P. Vogl for stimulating and helpful discussions.

[1] *Quantum Transport in Semiconductors*, edited by C. Jacoboni, L. Reggiani, and D. K. Ferry (Plenum, New York, 1992).
[2] D. K. Ferry, *Semiconductor Transport* (Taylor & Francis, London, 2000).
[3] See, e.g., S. M. Cho and H. H. Lee, J. Appl. Phys. **71**, 1298 (1992).
[4] M. Betz, S. Trumm, F. Sotier, A. Leitenstorfer, A. Schwanhäußer, M. Eckhardt, O. Schmidt, S. Malzer, G. H. Döhler, M. Hanson, D. Driscoll, and A. C. Gossard, Semicond. Sci. Technol. **19**, S167 (2004).
[5] For a review, see M. Reigrotzki, J. R. Madureira, A. Kuligk, N. Fitzer, R. Redmer, S. M. Goodnick, and M. Dür, Int. J. High Speed Electron. Syst. **11**, 511 (2001).
[6] R. Redmer, J. R. Madureira, N. Fitzer, S. M. Goodnick, W. Schattke, and E. Schöll, J. Appl. Phys. **87**, 781 (2000).
[7] J. R. Madureira, D. Semkat, M. Bonitz, and R. Redmer, J. Appl. Phys. **90**, 829 (2001).
[8] J. Bude, K. Hess, and G. J. Iafrate, Phys. Rev. B **45**, 10 958 (1992).
[9] S. Picozzi, R. Asahi, C. B. Geller, A. Continenza, and A. J. Freeman, Phys. Rev. B **65**, 113206 (2002).
[10] S. Picozzi, R. Asahi, C. B. Geller, and A. J. Freeman, Phys. Rev. Lett. **89**, 197601 (2002).
[11] M. Städele, J. A. Majewski, P. Vogl, and A. Görling, Phys. Rev. Lett. **79**, 2089 (1997).
[12] M. Städele, M. Moukara, J. A. Majewski, P. Vogl, and A. Görling, Phys. Rev. B **59**, 10 031 (1999).
[13] N. Fitzer, A. Kuligk, R. Redmer, M. Städele, S. M. Goodnick, and W. Schattke, Phys. Rev. B **67**, 201201(R) (2003).
[14] J. P. Perdew and A. Zunger, Phys. Rev. B **23**, 5048 (1981).
[15] N. Troullier and J. L. Martins, Phys. Rev. B **43**, 1993 (1991); **43**, 8861 (1991).
[16] L. Kleinman and D. M. Bylander, Phys. Rev. Lett. **48**, 1425 (1982).
[17] M. Stobbe, R. Redmer, and W. Schattke, Phys. Rev. B **49**, 4494 (1994).

[18] M. Reigrotzki, R. Redmer, N. Fitzer, S. M. Goodnick, M. Dür, and W. Schattke, J. Appl. Phys. **86**, 4458 (1999).
[19] M. V. Fischetti and S. E. Laux, Phys. Rev. B **38**, 9721 (1988).
[20] G. M. Dunn, G. J. Rees, J. P. R. David, S. A. Plimmer, and D. C. Herbert, Semicond. Sci. Technol. **12**, 111 (1997).
[21] See, for example, L. I. Schiff, *Quantum Mechanics* (McGraw-Hill, New York, 1968).
[22] Z. H. Levine and S. G. Louie, Phys. Rev. B **25**, 6310 (1982).
[23] P.-O. Löwdin, J. Chem. Phys. **19**, 1396 (1951).
[24] L. V. Keldysh, Zh. Eksp. Teor. Fiz. **37**, 713 (1959) [Sov. Phys. JETP **37**, 509 (1960)].
[25] N. Sano and A. Yoshii, Phys. Rev. B **45**, 4171 (1992).
[26] M. Reigrotzki, M. Stobbe, R. Redmer, and W. Schattke, Phys. Rev. B **52**, 1456 (1995).
[27] H. K. Jung, K. Taniguchi, and C. Hamaguchi, J. Appl. Phys. **79**, 2473 (1996).
[28] D. Harrison, R. A. Abram, and S. Brand, J. Appl. Phys. **85**, 8178 (1999); **85**, 8186 (1999).
[29] J. Kolnik, I. H. Oguzman, K. F. Brennan, R. Wang, and P. P. Ruden, J. Appl. Phys. **79**, 8838 (1996).
[30] E. Schreiber and H.-J. Fitting, J. Electron Spectrosc. Relat. Phenom. **131–132**, 87 (2003).